Journal of Power Sources 365 (2017) 92–97

Contents lists available at ScienceDirect

Journal of Power Sources

journal homepage: www.elsevier.com/locate/jpowsour

Short communication

Novel structure design of composite proton exchange membranes with continuous and through-membrane proton-conducting channels

Hang Wang [a, b], Chenxiao Tang [b], Xupin Zhuang [a, b, *], Bowen Cheng [a, **], Wei Wang [a], Weimin Kang [a, b], Hongjun Li [a]

[a] State Key Laboratory of Separation Membranes and Membrane Processes, Tianjin Polytechnic University, Tianjin, 300387, PR China
[b] College of Textile, Tianjin Polytechnic University, Tianjin, 300387, PR China

HIGHLIGHTS

- Novel PEMs with through-membrane proton-conducting channels are proposed.
- The structured PEMs were prepared via solution blowing and hot-pressed treatment.
- The effects of nanofiber distribution on the properties of PEMs were investigated.

GRAPHICAL ABSTRACT

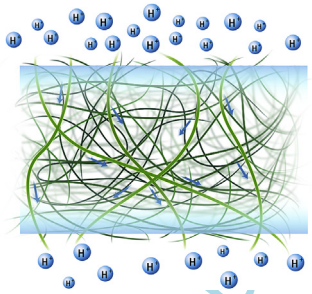

ARTICLE INFO

Article history:
Received 25 February 2017
Received in revised form
1 August 2017
Accepted 18 August 2017

Keywords:
Through-membrane
Proton exchange membrane
Hot-press
Solution blowing
Phenolphthalein sulfonated poly(ether sulfone)
Poly(vinylidene fluoride)

ABSTRACT

The primary goal of this study is to develop a high-performanced proton exchange membrane with the characteristics of through-membrane and continuous solution blown nanofibers as proton-conducting channels. The curled sulfonated phenolphthalein poly (ether sulfone) and poly (vinylidene fluoride) nanofibers were separately fabricated through the solution blowing process which is a new nanofiber fabricating method with high productivity, then they were fabricated into a sandwich-structured mat. Then this sandwich-structured mat was hot-pressed to form the designed structure using different melting temperatures of the two polymers by melting and making poly (vinylidene fluoride) flow into the phenolphthalein poly (ether sulfone) nanofiber mat. The characteristics of the composite membrane, such as morphology and performance of the membrane, were investigated. The characterization results proved the successful preparation of the membrane structure. Performance results showed that the novel structured membrane with through-membrane nanofibers significantly improved water swelling and methanol permeability, though its conductivity is lower than that of Nafion, the cell performance showed comparable results. Therefore, the novel structure design can be considered as a promising method for preparing of proton exchange membranes.

1. Introduction

At present, energy and environmental problems are the focuses of global concern. Direct methanol fuel cells (DMFCs) are considered to be a promising technology, because of their clean and

* Corresponding author. State Key Laboratory of Separation Membranes and Membrane Processes, Tianjin Polytechnic University, Tianjin, 300387, PR China.
** Corresponding author.
E-mail addresses: zhxupin@139.com (X. Zhuang), bowen15@tjpu.edu.cn (B. Cheng).

http://dx.doi.org/10.1016/j.jpowsour.2017.08.072
0378-7753/

efficient power sources [1]. As the core component of DMFCs, proton exchange membranes (PEMs) require superior proton conductivity, low methanol permeability and chemical stability [2]. For current DMFCs, PEMs comprising perfluorosulfonic acid polymers, such as Nafion, are the material of choice; however, perfluorosulfonic acid polymers show limited device lifetime caused by high methanol permeability and high swelling. Therefore, researchers have become motivated to overcome these issues and to improve PEM performances.

Extensive efforts were made to make some progress in some aspects. These efforts include (i) optimizing polymer structure [3–6], (ii) developing non-fluorinated ion conducting membranes to replace Nafion [2], and (iii) preparing blend membranes with various materials [7,8]. In recent years, designing stable PEMs chemically and mechanically while maintaining high ionic conductivity has been a requirement [3]. The development of nanofiber (NF) fabricating technology has resulted in the increase in the number of studies that focus on impregnating NFs into the polymer matrix to obtain high-performance PEMs; in this approach, NFs, which play the role of long channels for proton conduction, show better advantages than particle and rod-like additives because of their large length–diameter ratio [9,10]. It has been proven that protons could transport efficiently through hydrophilic ionic clusters along NFs through hopping, vehicular and surface transport in nanofiber composite membranes (NCMs) [11,12]. NFs decrease the methanol permeability by blocking methanol transmission pathway in the composite membranes as a methanol barrier layer [9]. The NFs in NCMs can form a three-dimensional network structure that has a good dimensional stability, and the swelling of membranes can be suppressed [13]. Many researchers [14,15] introduced different kinds of NFs into a matrix to fabricate membranes with nanofibrous skeleton, which showed property enhancement for composite membranes. Therefore, NFs play a major and positive role in PEMs [16–18].

According to the review of the related literature, the majority of these works were conducted by applying electrospun NFs to reinforce PEMs with impregnation [19,20]. Electrospinning is the main process used to prepare fibrous mat continuously with a high surface area and remarkable porosity [15,21]. However, the natural characteristics of the electrospinning process make NFs combine tightly to form a dense NFs network, which result in poor processability when NFs are used to reinforce PEMs through the impregnation process. The obtained composite membranes easily suffer from internal defects with some voids within composite structures [22]. Another serious structural defect is the unavoidable pure polymer layers at the surfaces of composite membranes [23,24]. This phenomenon indicates that the surface layers do not contain any NF, and these layers act as a “barrier layer” in proton transportation from one side to another side of PEMs. Thus, the distribution of NFs along the direction of membrane thickness must be improved.

In this work, we proposed a novel structure, which is shown in Fig. 1. We designed the NFs to build the transmembrane proton conduction path by distributing through PEMs; thus, protons could be transferred effectively and directly from one side to another side. Solution blowing process (SBP), which is a novel NF fabricating method, could be applied to achieve the proposed structure. In this process, polymer solutions are blown to ultrathin solution streams by a high-speed gas flow and solidify to NFs after solvents evaporation [25–29]. Unlike electrospun NFs, solution-blown NFs are commonly curled in three dimensions; this feature results in a loose construction [27,28]. Otherwise, a large number of crimped fibers are closely entangled to form a stable and entangled structure. Two different polymer NF mats were fabricated separately through SBP. Then, these polymer NF mats were constructed as a

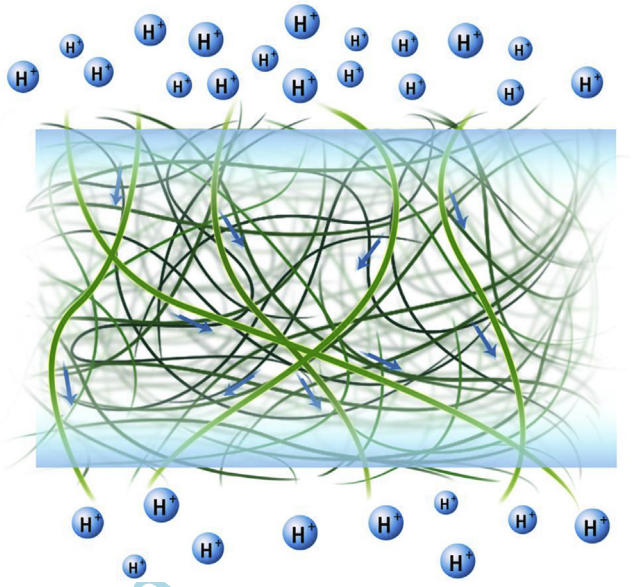

Fig. 1. Schematic representations of the structure of the designed membranes.

sandwiched structure. When an obvious difference existed in the melting temperatures of the two polymers and when the mat was hot-pressed over a low melting temperature, this kind of bicomponent NF mat could be converted to a dense membrane with curly NFs distributed, as designed in Fig. 1. In this study, hot-press treatment was used to melt polymer with a low melting temperature and to make this polymer flow into the void spaces between NFs with a high melting temperature. In brief, a novel PEM was designed by solution blowing of the two polymers with distinct melting temperature into the bicomponent NF mat, which was hot-pressed into a dense membrane with curly transmembrane NFs as proton conduction path.

With respect to polymer choice, sulfonated phenolphthalein poly (ether sulfone) (SPES-C) was selected as the high-melting point polymer. In recent years, sulfonated aromatic hydrocarbon polymers have been the focus of the development of novel polymer electrolyte membranes, such as sulfonated poly (ether ether ketone) (SPEEK) [30], sulfonated poly (ether sulfone) (SPES) [31], and sulfonated polyphenylsulfone (SPPSU) [32]. Phenolphthalein poly (ether sulfone) (PES-C) is a novel thermoplastic engineering material with phenolphthalein side chains. Thus far, PES-C has been the least reported among the various aromatic hydrocarbon polymers. SPES-C membranes have lower methanol permeability and higher resistance to swelling than conventional SPES membranes because of the rigidity of the main chains and the steric hindrance effect of phenolphthalein side chains [33]. Poly (vinylidene fluoride) (PVDF), which has a melting temperature of 172 °C, is a kind of low-melting point polymer that meets our structural design requirements. PVDF can be also used as melting components. Moreover, PVDF, which is a kind of hydrophobic material that can reduce methanol transport rate in PEMs [34], is commonly applied for fuel cells [35]. The PVDF with melting temperature lower than that of SPES-C, which is selected as low-melting point polymer and the methanol-resistant layer in this work. Furthermore, it can be used to foil the effects of through-membrane proton channels owing to the lack of ionic exchange capacity, and verify the successful construction of the structures of through-membrane proton-conducting channels. PVDF and SPES-C NF mats were first fabricated using the SBP separately. Then PVDF and SPES-C mats were made to a sandwiched structure, then compacted with

heating (180 °C, up to melting temperature of PVDF) to obtain membranes by allowing molten PVDF to flow into the void space. The rationale for this study was twofold: (i) We sought to design dense NCMs with through-membrane NFs, proton-conducting channels, and methanol-blocking layer. (ii) We sought to understand the effects of through-membrane NFs on the final membrane properties. The proton conductivity, swelling ratio, permeability of methanol, and mechanical property of PEMs were investigated.

We believe that hot-press NFs mat treatment was developed in this study as a route to prepare PEMs for the first time. This treatment simplifies the membrane fabrication procedure.

2. Experimental sections

2.1. Materials

PVDF was purchased from Solvay Co. PES was purchased from Changchun Institute of Applied Chemistry. *N*,N-dimethylformamide was procured from Tianjin Kermel Chemical Reagent Co. Ltd. All chemicals were of analytical grade.

2.2. Preparation of composite membrane

SBP is a new NF fabricating method with high productivity, and the experimental setup used to prepare nonwoven NFs was shown in our previous work [25]. The detailed synthetic method of SPES-C is shown in the supporting information (SI). Two polymer spinning solutions were prepared using *N*,*N*-dimethylformamide as solvents. PVDF and SPES-C NF mats were first fabricated through SBP separately. PVDF and SPES-C mats were constructed as a sandwiched structure composed of outer NF layers of SPES and a central base PVDF polymer layer. Then, these mats were preheated in a hot presser (CB-950Z5 hot-presser, China) at 180 °C without pressure. After 5 min, the multilayer mats were compacted by heating at 180 °C and a pressure of 10 MPa for 10 min. During hot pressing, the molten PVDF flowed into the void spaces between SPES-C NFs to create a fully dense membrane structure. Finally, the membrane was annealed at 180 °C. The weight-based compositions of PEMs (SPES-C/PVDF) were 80/20, 70/30, and 60/40 and were labeled as SPES-C/PVDF-20, SPES-C/PVDF-30, and SPES-C/PVDF-40, respectively. In addition, the membrane with pure PVDF on the surface and SPES-C NFs in the membrane was prepared for a comparison of conductivity and was labeled as SPES-C/PVDF-F. The thicknesses of all the composite membranes are approximately 150 μm.

2.3. Structural and morphological characterization of the nanofibers and composite membranes

The morphologies of the NFs and membranes were characterized using a scanning electron microscope (SEM; Hitachi S-4800), and the atomic force microscope (AFM) images were recorded in tapping mode (CSPM5500).

X-ray diffraction (XRD) measurements were performed via XRD spectroscopy (D8 Discover with GADDS).

2.4. Tensile strength

The tensile strength of dried membranes (dimensions: 1 cm × 4 cm) was measured using an Instron universal testing machine (3369, USA) at room temperature with a stretching rate of 2 cm/min. At least 3 specimens of each membrane were tested and the values were averaged.

2.5. Proton conductivity and Methanol permeability

The proton conductivity of the circular samples (dimensions: 1 cm) was measured by electrochemical impedance spectroscopy over the frequency range from 100 mHz to 100 kHz using an electrochemical workstation (CHI660D). The scheme of the setups of the through-plane conductivity is as described in Ref. [36]. In addition, the conductivity was measured at the relative humidity (RH) of 100% which was fixed for all the samples. The proton conductivity was calculated using the following formula: $\sigma = L{\cdot}A^{-1}\,R^{-1}$, where L, A, and R are the membrane thickness, cross-sectional area, and resistance of the membrane, respectively.

The methanol diffusion coefficients were calculated through formula variation of Fick's first law [37]: $DK = \frac{L \cdot V_B \cdot C_{B(t)}}{A \cdot C_{A(t-t0)}}$ where C_A and C_B are the methanol concentrations of methanol side (10 M) and water side, respectively; A, L, and V_B are the effective area, thickness of the membrane, and volume of the permeated compartment, respectively; DK is the methanol permeability; t is the end time, and t_0 is the start time. Methanol concentration was monitored by gas chromatography (Agilent 7820) equipped with a thermal conductivity detector (TCD) and a DB-624 column.

2.6. Single cell performance

5 mg/cm^2 Pt–Ru (1: 1) and 5 mg/cm^2 Pt–C were coated on the anode and cathode of membrane by electrostatic painting, respectively. Carbon papers (model: Xinyuan power), which were purchased from Kunshan Sunlaite Technology Limited (Jiangsu, China), were used as the gas diffusion layers. Then the single cell performance of each MEA was characterized by a DMFC testing station with single serpentine flow fields (FCTS, Arbin Inc., America) at 60 °C under 100% RH. The flow rate of the feeding fuel (2 M methanol aqueous solution) was 2 mL min^{-1}. The oxidant was oxygen at a flow rate of 0.5 L min^{-1}.

3. Results and discussions

3.1. Morphology of SPES-C and PVDF NFs

The SEM images of PVDF and SPES-C NFs are shown in Fig. 2(a) and (b). The corresponding diameter distribution maps are given in the SI (Fig. S1). SPES-C NFs with diameters ranging from 70 nm to 320 nm and PVDF NFs with diameters ranging from 50 nm to 250 nm were arranged in a disorderly manner. Fig. 2 shows that SPES-C and PVDF NFs were commonly curled in three dimensions and closely entangled. This observation indicated that SPES-C and PVDF NFs were obviously different from the electrospun NFs.

3.2. Structure of SPES-C/PVDF composite membranes

Fig. 3(a)–3(c) show the surface images of different NCMs. All of the membranes were completely compact with SPES-C NFs standing out of the PVDF matrix, which benefits the transport of protons. Fig. 3(a)–3(c) clearly show that the PVDF matrix encapsulates SPES-C NFs in the membrane. Furthermore, we could also determine the differences between each other. Fig. 3(a)–3(c) show that the content of PVDF led to a considerable change on the surface of composite membranes. The NFs on the surface of the membranes became sparse as the content of the PVDF increased. This result was consistent with the increase in the matrix. In particular, numerous PVDF matrices encapsulated SPES-C NFs thoroughly. A dense central base polymer layer was formed in the internal membranes. This layer is shown in Fig. 3(d) and (e). The NFs were well dispersed in the polymer matrix. The inner part showed a composite structure in which the NFs were dispersed in the PVDF matrix, thereby

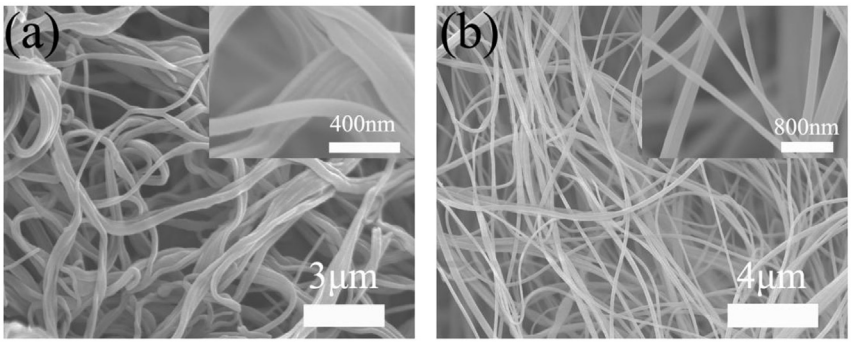

Fig. 2. SEM images of solution-blown (a) PVDF and (b) SPES-C NFs.

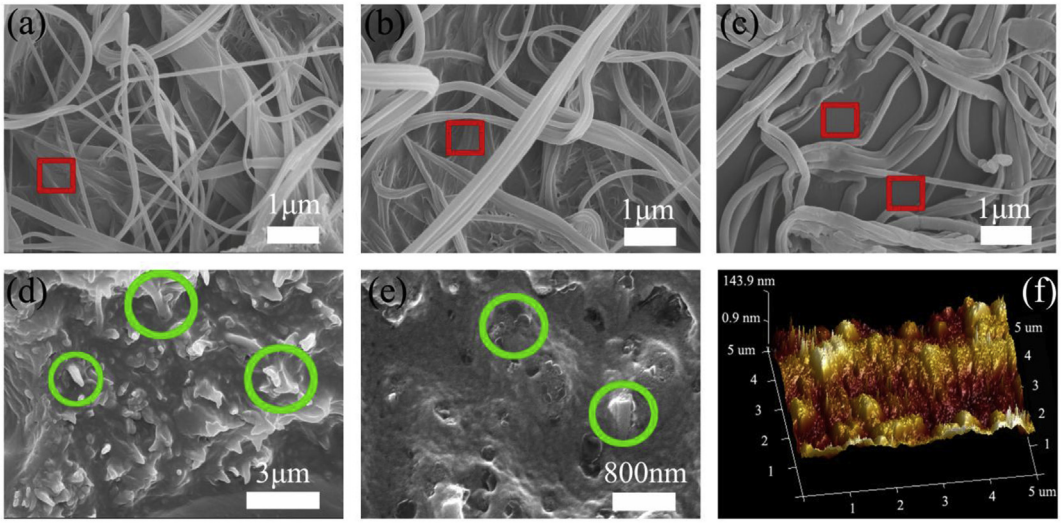

Fig. 3. SEM images of surfaces: (a) SPES-C/PVDF-20, (b) SPES-C/PVDF-30, (c) SPES-C/PVDF-40. (d) and (e) SEM images of cross-section of SPES-C/PVDF-20 (red and green pattern marked as PVDF matrix and SPES-C NFs, respectively), (f) AFM phase image of surface of SPES-C/PVDF-40. (For interpretation of the references to colour in this figure legend, the reader is referred to the web version of this article.)

ensuring the continuous channel for proton conduction. The PVDF formed a continuous methanol-resistant layer by flowing into the void spaces of SPES-C NFs. The sectional images of the different locations of NCMs showed different distribution directions of the NFs in the membrane. This observation revealed that the solution-blown NFs are commonly curled in three dimensions. This condition is helpful to improve proton conductivity and dimensional stability.

Fig. 3(f) shows that the AFM phase images in the tapping mode of membrane surfaces presented a bright/dark nanophase-separated morphology, with the dark regions representing the hydrophilic domains [38,39]. These domains absorbed water and facilitated the transport of water and protons, whereas the bright regions corresponding to the hydrophobic domains provided methanol resistance and dimensional stability in the membranes. The phenomenon also revealed that the hydrophilic phase domains were apparently well connected to form proton channels, and the NFs were dispersed in the PVDF matrix to form dense membrane.

The XRD curves of all the samples are shown in Fig. 4(a). The peak of SPES-C was flat and occurred at 2θ of 17.6°. The peak of NCMs mainly occurred at 2θ of 18.46°, 20°, 26.72°, and 39°, and the PVDF showed a wide dispersion peak around 21° which indicted a low degree of crystallinity. However, the peaks of NCMs remained sharp at approximately 20°. The reason is that, after the hot-press treatment, the NCMs showed a high degree of crystallinity, which corresponded to 200/110 reflections of the β-phase, and weak peaks at approximately 18.2° and 27.2°, which corresponded to 020 and 111 reflections of the α-phase, respectively [25]. This phenomenon indicated that the PVDF in the internal membranes was a continuous layer that could block methanol crossover. Besides, the peaks for NCMs also showed flat with the increasing content of SPES-C. This result was caused by the SPES-C redistribution in the PVDF. This result also revealed the good compatibility of the materials.

3.3. Tensile strength

The mechanical properties of different membranes and SPES-C NFs are shown in Fig. 4(e). All composite membranes had excellent mechanical properties compared to PVDF membrane. Moreover, the mechanical performance of the composite membranes initially increased and then decreased with the increase in the PVDF content. This phenomenon occurred mainly because the matrix could not connect NFs when the content of PVDF was low. By contrast, when the content of PVDF was high, NFs could not reinforce the membranes well. Hot-press treatment could improve the mechanical property of the PEMs [40]. Dimensional stability, oxidative stability and selectivity of different membranes are shown in SI.

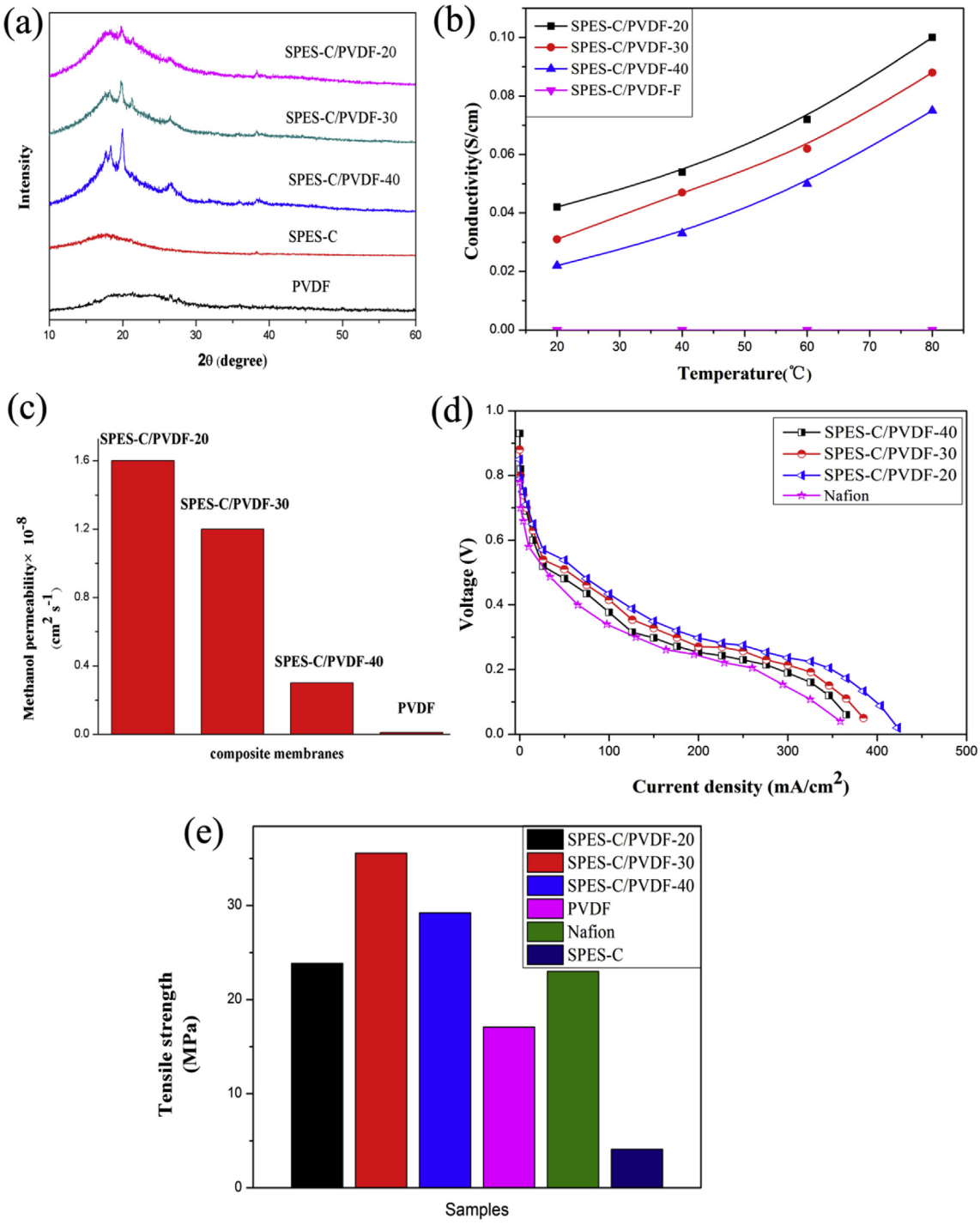

Fig. 4. (a) XRD curves; (b) proton conductivity at varying temperatures under 100% RH; (c) methanol permeability; (d) single cell performances at 60 °C under 100% RH; and (e) mechanical properties of all the samples.

3.4. Proton conductivity and Methanol permeability

Proton conductivity and methanol permeability of all the NCMs are summarized in Fig. 4(b) and (c), respectively. Proton conductivity was measured at varying temperatures (i.e., 20 °C–80 °C, 100% RH). The plots of conductivity showed that the conductivity of the novel designed membranes exhibited positive dependency with temperature. This finding revealed that proton conduction is a thermally activated process. Fig. 4(b) shows that the proton conductivity of SPES-C/PVDF-F was the lowest and close to 0. However, the proton conductivities of the membrane with through-membrane NFs were all higher than those of SPES-C/PVDF-F. These proton conductivities could obtain 0.1 S cm^{-1} at 80 °C under 100% RH (SPES-C/PVDF-20). However, the proton conductivity of SPES hybrid membrane prepared by Wen was only 0.047 S/cm under the same condition [41]. Therefore, the through-membrane and continuous SPES-C NFs extended from one side to another side of the membrane can provide benefits. The proton

conductivities decreased with the increase in the content of PVDF. This finding revealed that the decrease in the surface distribution of the NFs results in the gradual encapsulation of conduction channels by the PVDF matrix. Therefore, the existence of the "barrier layer" of proton transportation at the surface of membranes hindered proton transport and NFs can form proton-conducting channels in the membrane to improve the proton conductivity. The methanol permeabilities of all the NCMs and Nafion were measured at room temperature. The methanol permeabilities of all the NCMs were very low and could be as low as 1/500 that of Nafion117 (14.1×10^{-7} cm^2 s^{-1}). The increase in the content of SPES-C NFs resulted in the increase in methanol permeability. The probable reason is that the methanol resistance layers of PVDF became slightly efficient because of the decrease in the content of the PVDF matrix. Therefore, the presence of PVDF successfully hinders methanol crossover.

3.5. Single cell performance

Fig. 4(d) shows the polarization curves of the single cells fabricated by the composite membranes at 60 °C and 100% RH. The cell performances of the composite membranes decreased with the increase of PVDF contents. Furthermore, at the current density of 100 mA/cm^2, the output voltages of SPES-C/PVDF-20, SPES-C/PVDF-30, and SPES-C/PVDF-40 are measured as 0.37692, 0.41538, and 0.43385 V, respectively, while that of Nafion is only 0.35 V or lower [42–44]. All their sing cell performances have competitive advantage compared to Nafion.

4. Conclusion

In this study, we reported a novel approach to prepare composite PEMs with through-membrane and continuous nanochannels and methanol-blocking layer through SBP and hot-press treatment. The existence of the "barrier layer" of proton transportation at the surface of membranes could hinder proton transport and NFs on surface can form proton-conducting channels in the membrane improve the proton conductivity. The through-membrane NFs significantly improved the proton conductivity and cell performance of the PEMs. The mechanical performance of composite membranes initially increased and then decreased with the increase in the PVDF content. The composite membranes were effective in hindering methanol permeability because of the presence of the continuous methanol-blocking layer, and the cell performance of composite membrane showed comparable results compared to Nafion. A substantial decrease in SR occurred. The SRs of all the composite membranes were less than 10%, and the membranes exhibited improved dimensional stability when SPES-C NF is incorporated into the PVDF matrix. The results revealed that the novel structure design can be considered a novel route to prepare high-performance and cost-effective membranes for DMFC applications.

Acknowledgements

The author would like to thank National Natural Science Foundation of China (51473121), National Key R&D Plan (2016YFB0303304), the Science and Technology Plans of Tianjin (15PTSYJC00230, 13JCYBJC16700 and 14TXGCCX00014), National science and technology support program (2015BAE01B03), the Fund Project for Transformation of Scientific and Technological Achievements from Jiangsu Province (BA2015182), and the Program for Changjiang Scholars and Innovative Research Team in University (PCSIRT) of Ministry of Education of China (Grand no. IRT13084) for their financial supports.

Appendix A. Supplementary data

Supplementary data related to this article can be found at http://dx.doi.org/10.1016/j.jpowsour.2017.08.072.

References

[1] S.J. Peighambardoust, S. Rowshanzamir, M. Amjadi, Int. J. hydrogen Energy 35 (2010) 9349–9384.
[2] V. Neburchilov, J. Martin, H. Wang, J. Zhang, J. Power Sources 169 (2007) 221–238.
[3] S.G. Chalk, J.F. Miller, J. Power Sources 159 (2006) 73–80.
[4] H. Li, G. Zhang, J. Wu, C. Zhao, Y. Zhang, K. Shao, M. Han, H. Lin, J. Zhu, H. Na, J. Power Sources 195 (2010) 6443–6449.
[5] K. Yoshimura, K. Iwasaki, Macromolecules 42 (2009) 9302–9306.
[6] F. Zhang, N. Li, S. Zhang, S. Li, J. Power Sources 195 (2010) 2159–2165.
[7] M. Divona, Z. Ahmed, S. Bellitto, A. Lenci, E. Traversa, S. Licoccia, J. Membr. Sci. 296 (2007) 156–161.
[8] R.K. Nagarale, G.S. Gohil, V.K. Shahi, J. Membr. Sci. 280 (2006) 389–396.
[9] I. Shabani, M.M. Hasani-Sadrabadi, V. Haddadi-Asl, M. Soleimani, J. Membr. Sci. 368 (2011) 233–240.
[10] H. Li, Y. Liu, J. Mater. Chem. A 2 (2014) 3783–3793.
[11] S. Zhang, G. He, X. Gong, X. Zhu, X. Wu, X. Sun, X. Zhao, H. Li, J. Membr. Sci. 493 (2015) 58–65.
[12] H. Wang, X. Li, X. Zhuang, B. Cheng, W. Wang, W. Kang, L. Shi, H. Li, J. Power Sources 340 (2017) 201–209.
[13] X. Xu, L. Li, H. Wang, X. Li, X. Zhuang, RSC Adv. 5 (2015) 4934–4940.
[14] S. Shahgaldi, M. Ghasemi, W.R. Wan Daud, Z. Yaakob, M. Sedighi, J. Alam, A.F. Ismail, Fuel Process Technol. 124 (2014) 290–295.
[15] C. Lee, S.M. Jo, J. Choi, K. Baek, Y.B. Truong, I.L. Kyratzis, Y. Shul, J. Mater. Sci. 48 (2013) 3665–3671.
[16] B. Zhang, X.P. Zhuang, B. Cheng, N. Wang, Y. Ni, Mater Lett. 115 (2014) 248–251.
[17] R. Takemori, H. Kawakami, J. Power Sources 195 (2010) 5957–5961.
[18] J.D. Snyder, Y.A. Elabd, J. Power Sources 186 (2009) 385–392.
[19] R. Sood, S. Cavaliere, D.J. Jones, J. Rozière, Nano Energy 26 (2016) 729–745.
[20] J. Lee, N. Kim, M. Lee, S. Lee, J. Membr. Sci. 367 (2011) 265–272.
[21] S. Yun, J. Woo, S. Seo, L. Wu, D. Wu, T. Xu, S. Moon, J. Membr. Sci. 367 (2011) 296–305.
[22] U. Stachewicz, F. Modaresifar, R.J. Bailey, T. Peijs, A.H. Barber, ACS Appl. Mater. Inter 4 (2012) 2577–2582.
[23] D.M. Yu, S. Yoon, T. Kim, J.Y. Lee, J. Lee, Y.T. Hong, J. Membr. Sci. 446 (2013) 212–219.
[24] M.M. Hasani-Sadrabadi, I. Shabani, M. Soleimani, H. Moaddel, J. Power Sources 196 (2011) 4599–4603.
[25] L. Shi, X. Zhuang, X. Tao, B. Cheng, W. Kang, Fiber Polym. 14 (2013) 1485–1490.
[26] S. Shi, X. Zhuang, B. Cheng, X. Wang, J. Mater. Chem. A 1 (2013) 13779.
[27] X. Zhuang, K. Jia, B. Cheng, X. Feng, S. Shi, B. Zhang, Chem. Eng. J. 237 (2014) 308–311.
[28] X. Zhuang, X. Yang, L. Shi, B. Cheng, K. Guan, W. Kang, Carbohyd. Polym. 90 (2012) 982–987.
[29] H. Wang, X. Zhuang, J. Tong, X. Li, W. Wang, B. Cheng, Z. Cai, J. Appl. Polym. Sci. 132 (2015) 42843.
[30] K. Chae, K. Kim, M. Choi, E. Yang, I.S. Kim, X. Ren, M. Lee, Chem. Eng. J. 254 (2014) 393–398.
[31] S. Chul Gil, J. Chul Kim, D. Ahn, J. Jang, H. Kim, J. Chul Jung, S. Lim, D. Jung, W. Lee, J. Membr. Sci. 417-418 (2012) 2–9.
[32] B. Decker, C. Hartmann-Thompson, P.I. Carver, S.E. Keinath, P.R. Santurri, Chem. Mater 22 (2010) 942–948.
[33] L. Jia, X. Xu, H. Zhang, J. Xu, J. Polym. Sci. B Polym. Phys. 35 (1997) 2133–2140.
[34] M.S. Subramanian, G. Sasikumar, J. Appl. Polym. Sci. 117 (2010) 801–808.
[35] S. Ren, G. Sun, C. Li, Z. Wu, W. Jin, W. Chen, Q. Xin, X. Yang, Mater. Lett. 60 (2006) 44–47.
[36] T.D.O. Gadim, F.J.A. Loureiro, C. Vilela, N. Rosero-Navarro, A.J.D. Silvestre, C.S.R. Freire, F.M.L. Figueiredo, Electrochim. Acta 233 (2017) 52–61.
[37] J. Zhang, Z. Zhou, Chin. J. Power Sources 31 (2007) 721–724.
[38] W.H. Lee, K.H. Lee, D.W. Shin, D.S. Hwang, N.R. Kang, D.H. Cho, J.H. Kim, Y.M. Lee, J. Power Sources 282 (2015) 211–222.
[39] D.W. Shin, S.Y. Lee, N.R. Kang, K.H. Lee, D.H. Cho, M.J. Lee, Y.M. Lee, K.D. Suh, Int. J. Hydrogen Energ 39 (2014) 4459–4467.
[40] J.B. Ballengee, P.N. Pintauro, J. Membr. Sci. 442 (2013) 187–195.
[41] S. Wen, C. Gong, Y. Shu, F. Tsai, J. Yeh, J. Appl. Polym. Sci. 123 (2012) 646–656.
[42] H. Lin, S. Wang, J. Membr. Sci. 452 (2014) 253–262.
[43] H.S. Thiam, W.R.W. Daud, S.K. Kamarudin, A.B. Mohamad, A.A.H. Kadhum, K.S. Loh, E.H. Majlan, Energ. Convers. Manag. 75 (2013) 718–726.
[44] H. Ahmad, S.K. Kamarudin, U.A. Hasran, W.R.W. Daud, Int. J. Hydrogen Energ 36 (2011) 14668–14677.